THE ASTROPHYSICAL JOURNAL, 365:L19–L22, 1990 December 10

A ROTATING, EXPANDING DISK IN THE WOLF-RAYET STAR EZ CANIS MAJORIS?

R. E. SCHULTE-LADBECK, K. H. NORDSIECK, M. A. NOOK, A. M. MAGALHÃES, M. TAYLOR,
K. S. BJORKMAN, AND C. M. ANDERSON
Space Astronomy Laboratory, The University of Wisconsin at Madison
Received 1990 July 23; accepted 1990 September 26

ABSTRACT

We report the discovery of linear polarization changes across the extended wings of He II lines, mainly the strong 4–3 transition at 4686 Å, in the WN5 star EZ CMa. When the polarization across the line profiles is plotted in the Stokes parameter plane, it traces loops clockwise from the blue wing through line center to the red, rather than straight lines. Such polarization loops are reminiscent of what is observed in the Balmer lines of Be stars. We propose that the continuum polarization in EZ CMa can be understood by an axisymmetric, electron-scattering envelope, with the decrease in polarization in He II being caused by an increase in absorptive opacity in the lines and dilution by unpolarized line emission, while the variations in position angle are due to the Doppler-shifted absorptive opacity and/or scattered line photons. As the sense of rotation in the loops is also independent of phase of this alleged Wolf-Rayet + compact binary, we speculate that the polarized line profiles are the signature of a rotating, expanding wind geometry around a single star.

Subject headings: line profiles — polarization — stars: individual (EZ Canis Majoris) — stars: Wolf-Rayet

I. INTRODUCTION

Wolf-Rayet stars are generally believed to be evolved, luminous stars which lose mass via strong stellar winds. While there is ample observational evidence for the presence of winds, the physical mechanism(s) responsible for driving the expansion of W-R star atmospheres has not yet been established. Some W-R winds suffer from a momentum problem, i.e., the momentum in the outflowing matter seems to exceed significantly the photon momentum of the radiation field. Consequently, additional forces may be needed to enhance the winds of W-R stars if they are to be described within the framework of the radiation-driven wind theory developed by Castor, Abott, and Klein (1975) for O stars.

It may be possible to explain the winds of some WN stars by adopting increased stellar luminosities (e.g., Pauldrach *et al.* 1985). An alternative approach by Poe, Friend, and Cassinelli (1989) incorporates the effects of stellar rotation and corotating magnetic fields. These models require that W-R stars are rapid rotators, spinning close to break-up velocity. As the winds of W-R stars are optically thick and even the continuum is formed in an extended region (Hartmann and Casinelli 1977), it should be difficult to detect rotation by the conventional observational methods, i.e., by measuring the widths of photospheric absorption lines. The magnetic rotator model implies, however, that the winds of W-R stars are differentially rotating and axisymmetric, with a slower but denser equatorial flow and a fast wind at higher latitudes. The shape of the winds may thus carry information on their driving mechanism. Maeder (1987) calculated one evolutionary track with rotationally induced mixing; it can reproduce the position of W-R stars in the H-R diagram.

The first indication that the wind geometry of EZ CMa deviates from spherical symmetry came from the detection of intrinsic linear polarization by Serkowski (1970). Cassinelli and Haisch (1974) then modeled the polarization of rotationally distorted, electron-scattering atmospheres and explained the observed polarization with a disk-shaped geometry. Polarization structure was detected across the spectrum by McLean *et al.* (1979), revealing the existence of stratification of ionization, the He II recombination lines being formed deeper in the wind than those of He I in an envelope that is highly ionized and/or hydrogen-deficient and flattened, with additional time variations suggesting a nonsteady, non–axially symmetric phenomenon. Circular polarization measurements (McLean *et al.* 1979; Drissen *et al.* 1989) indicate a (longitudinal) field of less than a few hundred G.

The variability of EZ CMa is not understood. The He II λ4686 line shows a variable velocity, flux, and transient asymmetries in its profile (Wilson 1948); the optical continuum is variable (Kuhi 1967), as is the linear polarization (McLean 1980). While a number of time scales from hours to days are apparent in the observations, a periodicity of about 3.8 days occurs in many optial data sets. The discussion of binary motion versus pulsational modulation versus rotation has thus raged through the literature. Firmani *et al.* (1980), advocating the binary hypothesis, showed that the companion to the WN5 star should be a neutron star. Drissen *et al.* analyzed optical photometry and polarimetry and favor binary modulation in conjunction with another, sporadic phenomenon. Willis *et al.* (1989) were unable to detect periodic variations in the UV P Cygni profiles, i.e., the Hatchett and McCray effect, but noticed epochs of relative quiescence and activity considered intrinsic to the W-R wind. In order to reconcile their data with the optical periodicity, they suggested rotation, with an additional "activity" mechanism.

II. INSTRUMENTATION AND OBSERVATIONS

In this *Letter*, we present a new type of observation, He II polarization profiles, those of the He II λ4686 line in particular. The data were obtained with the spectropolarimeter on the 36 inch (0.9 m) telescope of the Pine Bluff Observatory of the University of Wisconsin. The instrument measures the three Stokes parameters Q, U, and I simultaneously over the spectral range 3200–7800 Å. The polarization optics and camera were designed by Nordsieck (1987, 1991). The maximum instrumental efficiency occurs between 4500 and 5000 Å, which greatly

aided in detecting the line effects in He II λ4686. We used a plane 300 lines mm^{-1} grating which yields a dispersion of 5 Å $pixel^{-1}$. This provides a spectral resolution of ~34 Å FWHM with the 12″ entrance aperture.

We usually observed three flux standards per night. The polarimetric stability of the system was monitored by observing unpolarized and highly polarized standard stars roughly once per week. Using a baseline of several months, we have determined that the instrumental variability is less than 0.005%, and the nightly error in the polarimetric efficiency is smaller than 1 part in 100. Therefore, our systematic errors should not be greater than 0.01%. We also note that polarization measurements of comparison sources did not show the line-polarization effects discussed in this *Letter*, and we therefore rule out instrumental effects such as scattering in the spectrograph.

A journal of observations is given in Table 1; we also indicate the phases (Lamontagne, Moffat, and Lamarre 1986). The polarization integrated over the entire spectrum is listed (percentage polarization, 1 σ error, and equatorial position angle) for comparison with filter-polarization data.

III. RESULTS

The integrated polarizations agree well with filter observations obtained in the spring of 1990 by Robert *et al.* (1990). In particular, all data sets show only one pronounced polarization peak around phase 0.8–0.9, with a fairly large amplitude. Note that binary modulation usually produces two phase peaks in the polarization.

In Figure 1, we selected a segment of the (March 3) spectrum from 4000 to 5500 Å to illustrate the line-polarization effects. The drop in percentage polarization in the lines of He II λ4542, N V λλ4604, 4620, N III λ4640, He II λ4686, He II λ4860, and He II λ5412 is very pronounced, as is the associated change in the position angle. (Note that much of the position angle variation in this figure is due to interstellar polarization). Our data compare well with the polarization spectrum of McLean *et al.*, which was also obtained at a high, ~1%, level of continuum polarization. Figure 1 is centered on the strong and very broad line of He II λ4686. There is obvious polarization structure across the line profile. The extrema of polarization occur on the blue side of the spectral line peak.

The new line polarization effects reported here are revealed when one plots the normalized linear Stokes parameters for each night across the He II λ4686 line in a *Q*, *U* diagram. The *Q*, *U* diagrams of all nights show an elliptical pattern or *looping* as a function of wavelength. The sense in which these loops are traced with wavelength, clockwise from blue to the red across the line profile, is the same for each night. (Note that if the loops were a chance detection, one would expect random directions of the rotation).

TABLE 1

JOURNAL OF OBSERVATIONS

Date (1990)	JD 2,440,000+	Phase	*P*	*dP*	PA
Feb 5	7,925.6797	0.54	0.55%	0.01%	138°
Feb 20	7,942.6582	0.05	0.542	0.009	139
Feb 21	7,943.6318	0.31	0.48	0.01	138
Feb 25	7,947.6071	0.37	0.461	0.008	144
Feb 28	7,950.5957	0.16	0.58	0.02	138
Mar 2	7,952.6225	0.70	0.74	0.01	153
Mar 3	7,953.6074	0.96	0.87	0.01	139

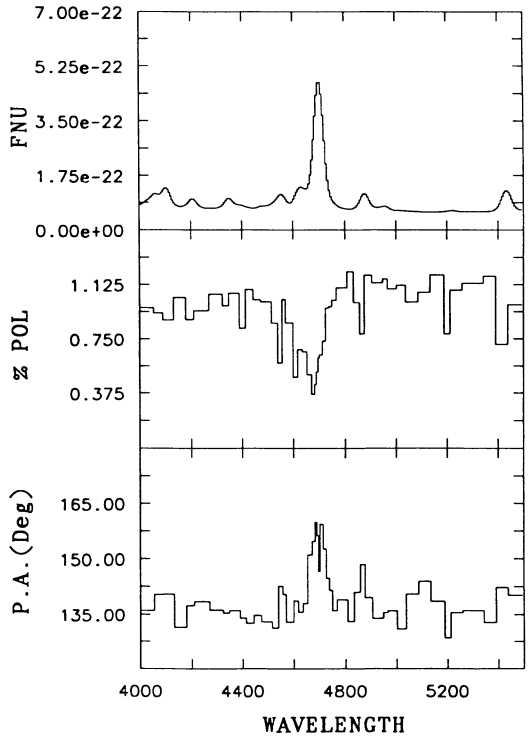

FIG. 1.—Observed spectropolarimetry of EZ CMa on 1990 March 3 centered on the He II λ4686 line. The flux in ergs cm^{-2} s^{-1} Hz^{-1}, degree of linear polarization in percent, and equatorial position angle in degrees are plotted as a function of wavelength in Å. The S/N in the polarization is ~10. Note the strong polarization feature associated with the He II line.

In order to increase the S/N ratio of the observations, we combined the polarimetric data of the five February nights which had very similar polarizations. We then subtracted an interstellar foreground polarization determined from simultaneous fits of a Serkowski-type law to the continuum polarization of all nights and the direction of the line polarization. The parameters are $P_{max} = 0.55\%$ ($\lambda_{max} = 5500$ Å) at a position angle of 0°. This does not affect the shape of the *Q*, *U*-plane polarization line profile, since the color of interstellar polarization is negligible over such a small wavelength range.

The combined *Q*, *U* parameters as a function of wavelength across He II λ4686 are displayed in Figure 2*a*. The line width was measured in the (combined) flux spectrum. The line center occurs at 4696 Å, and the red wing extends to ~4815 Å, taken as the minimum between He II λ4686 and He II λ4860 where the flux (almost) reaches an interpolated continuum level. Since the He II λ4686 line is severely blended on the blue wing with N V and N III, we defined a blue continuum well outside of these lines, from ~4420 to 4455 Å, and integrated the polarization in this "filter." The bluest point of the line profile was taken at 4653 Å, the observed flux minimum between the N III λ4640 and the He II λ4686 line. The polarization across the He II line was then binned to a nominal error of ≤0.035% polarization. The values are given in Table 2.

We can see in Figure 2*a* that the polarization decreases through the He II λ4686 line by ~0.3%. The intrinsic line polarization points back to the origin of the *Q*, *U* diagram, as expected after correction for interstellar polarization. Note that the line polarization does not go to the value anticipated for pure dilution by unpolarized line flux. If the interstellar polarization was correctly removed, this indicates that the line

TABLE 2

INTRINSIC POLARIZATION/BIN THROUGH He II λ4686

λ1 (Å)	λ2 (Å)	Q	U	dP	P	PA
4419.0	4455.0	−0.575%	−0.578%	0.039%	0.815%	112°.58
4653.0	4671.0	−0.367	−0.322	0.033	0.488	110.60
4671.0	4683.0	−0.245	−0.283	0.025	0.374	114.54
4683.0	4689.0	−0.244	−0.301	0.031	0.387	115.50
4689.0	4695.0	−0.228	−0.360	0.028	0.426	118.83
4695.0	4701.0	−0.223	−0.403	0.031	0.461	120.55
4701.0	4707.0	−0.229	−0.431	0.034	0.488	121.02
4707.0	4719.0	−0.220	−0.466	0.030	0.515	122.38
4719.0	4737.0	−0.346	−0.518	0.032	0.623	118.14
4737.0	4761.0	−0.449	−0.523	0.034	0.689	114.66
4761.0	4797.0	−0.484	−0.451	0.034	0.661	111.51
4797.0	4809.0	−0.582	−0.521	0.064	0.782	110.91

NOTE.—The first bin represents the blue continuum point.

photons themselves are being polarized by subsequent electron scattering. We also note that the line center does not coincide with the minimum in polarization. This could either reflect uncertainty in the interstellar polarization correction or, since the line seems to show this asymmetry also in the uncorrected data of individual nights, could be due to underlying P Cygni absorption on the blue side of the profile or additional scattered emission on the red wing. However, the important feature in Figure 2*a* is the huge width of the He II λ4686 polarization loop, measuring about 0.2%. We also find indications for polarization loops across He II λ5412 and λ6560, but the S/N is still very low even in the combined data.

In Figure 2*b*, we display the combined flux, corrected polarization, and position angle spectra. We overplotted in the top panel the spectrum of the polarized flux, $P \times$ FNU. The continuum levels of the polarized flux and the flux spectrum were matched to faciliate comparing relative line strengths. We note that all polarized flux lines show a redshift of the line peaks with respect to the spectral line peaks. Also, the slope of the He II λ4686 blue wing is very steep, whereas the red wing is broadened by what looks like a "shoulder" on the red side of the profile. Finally, there is residual position angle variation across the line that reflects the *Q*, *U* loop in Figure 2*a*.

IV. DISCUSSION

We focus our discussion on the polarization loops (the character of the spectropolarimetric variability will be discussed elsewhere). The presence of intrinsic polarization in EZ CMa indicates a deviation from spherical symmetry in the illuminator/scatterer geometry. As the continuum and the line polarization vectors (to first order) point in the same direction, the overall geometry of the envelope appears to be axisymmetric. Consider hence as a simple, qualitative model the continuum polarization originating from a static, axisymmetric, purely electron-scattering envelope. Since the Thomson-scattering cross section is independent of wavelength, the polarization will be constant as a function of wavelength, as the envelope has only one symmetry plane, the position angle

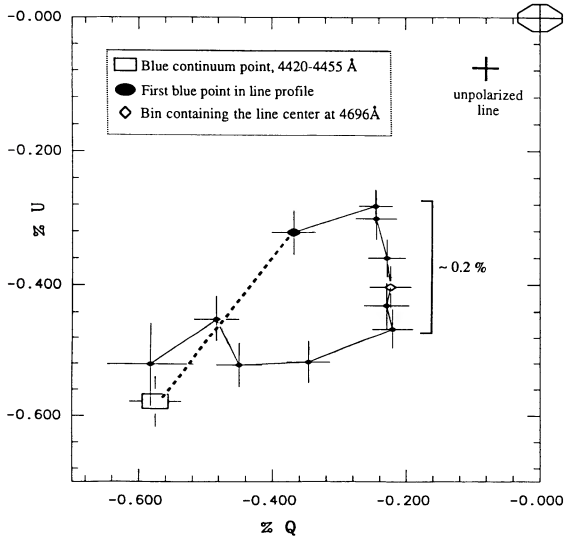

FIG. 2*a*

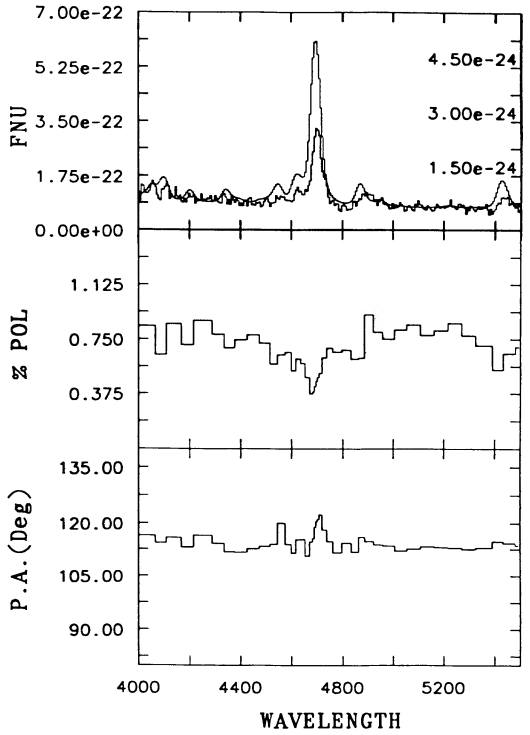

FIG. 2*b*

FIG. 2.—(*a*) The data for several nights were combined to increase the S/N and were corrected for interstellar polarization to reveal the intrinsic polarization of EZ CMa. The Stokes parameters *Q* and *U* in percent are displayed as a function of wavelength across the He II λ4686 line. The line center is indicated by an open diamond, the blue continuum by an open rectangle, and the first bin on the blue side of the profile by a larger dot. The error bars are 1 σ errors. The dashed line between the blue continuum point and the first blue point in the line represents a linear interpolation of the Stokes parameters for this wavelength region since the blue wing of the He II line is blended with nitrogen lines. The polarization decreases through the line, by ~0.3%, but also shows a component nonparallel to the depolarization direction, of about 0.2%; thus, the polarization "loop" traced clockwise from blue to red. Although the line polarization decreases toward the origin (*open octahedron*) of the *Q*, *U* diagram, it does not reach the value expected from pure dilution by unpolarized emission (*cross*). An asymmetry with respect to the line center is apparent which might be due to underlying P Cygni absorption in the blue wing or added scattered emission on the red wing. (*b*) The flux, polarization, and position angle for the combined and corrected data set are displayed with the same scaling as in Fig. 1. The polarization is binned to the same error as in (*a*). In the top panel we also show the polarized flux (use the scale on the right side). The He II λ4686 line is a strong feature in polarized flux indicating that the line photons are themselves scattered in the wind. Note that the blue wing of the polarized line profile is steeper than the red wing, which seems to have a "shoulder" added on to it that is not visible in the spectral line profile. Note also that the peaks of all polarized lines are redshifted with respect to the spectral line peaks.

will also be constant; the polarization is represented by a point in the Q, U plane. Consider now the presence in this envelope of an emission line that emits unpolarized line photons. If the photons escape without subsequent scattering, the effect on the continuum polarization is a depolarization through dilution. This produces a straight line pointing to the origin of the Q, U diagram that scales with the line strength. For the combined He II λ4686 line data of EZ CMa with the line being about 7 times the continuum flux, we expected the polarization to go to one-seventh of the continuum value (Fig. 2*a*, *cross*). Apart from showing residual line polarization, the position angle also changes through the line profile, resulting in the Q, U loop. We conclude that the geometry as seen by an observer in the line wings is not axially symmetric.

Detected here for the first time in a W-R star, polarization loops have previously been reported in the emission lines of two other types of astronomical objects, in Be stars (e.g., Poeckert and Marlborough 1978) and in SN 1987A (Cropper *et al.* 1988). These have some properties in common, such as a nonspherical, electron-scattering atmosphere, expansion of the wind, and rotation of the star. While there is as yet no detailed model available for the line polarization in SN 1987A, Poeckert and Marlborough successfully modeled the Balmer-line polarization loops and spectral-line profiles of the Be star γ Cas, with a partially ionized, rotating, expanding, and inclined disk. The modification of the polarization across the lines is shown to be primarily due to line absorption and, to a lesser extent, dilution by emission. In the blue line wing, for example, the (polarized) continuous flux from the approaching part is strongly attenuated by line absorption, while we see deeper into the receding part since the absorbing atoms are receding from the observer and line absorption of continuous flux occurs only for the red wing. We consequently see a different spatial integration over the envelope in scattered light for the blue and red wing, which is an integration over a volume that is in general no longer axisymmetric. The sense of rotation of the polarization loops in this model reflects the direction of rotation of the star/envelope. We also note that the spectral-line profiles in Be star models may look very much like P Cygni profiles for high inclinations. According to the model of EZ CMa by Hillier (1987), the He II 4–3 transition is optically thick, i.e., it absorbs continuum photons. We can therefore consider the Be star model applicable to EZ CMa.

In the case of Wolf-Rayet stars, an additional effect that could give rise to polarization loops is the scattered emission itself. It is of interest to note that electron scattering is also considered to produce the extended red wings of He II spectral line profiles of EZ CMa (Hillier 1984). Which process is prevalent in EZ CMa, Doppler-shifted absorption, or scattered emission, can be tested by searching for polarization loops in lines of different absorption optical depth and ionization potential.

Let us finally consider whether the polarization loops might be accounted for instead by a binary model for EZ CMa, and assume that the He II line is formed mostly in an ionization wake trailing behind the neutron star orbiting around in the expanding wind of the W-R star. The binary geometry is axisymmetric, and the line polarization may display depolarization through dilution by emission. A difference in the geometrical location of the blue and red wing of the emission lines could arise if the ionization wake were extended along the orbit, thus giving different scattering angles in the blue and red wing of the line as the line flux scatters off denser parts of the W-R wind. However, on one side of the orbit the head of the ionization wake will be coming toward us and hence be blue-shifted, while on the other side, it will be moving away from us. We would thus expect the polarization to loop in opposite directions for opposite orbital phases. Instead, our observations show that the polarization loops are always traced in the same sense independent of orbital phase.

Polarization structure may be expected to be present in any Doppler-broadened emission-line/shell absorption feature arising in an oblate, axisymmetric envelope undergoing large dynamical motions; the emission/absorption acts as a depolarizing agent and selects flux from different parts of the envelope. The similarities in the polarization of Be stars, SN 1987A, and the W-R star EZ CMa thus exemplify the common physical processes occurring in dynamical circumstellar plasmas of high electron density. The atmospheres of W-R stars are extremely difficult to model, and the discovery of polarization loops adds a new complexity. Absorption, emission, and scattering all play a significant role in the formation of the (polarized) line profiles. It is of importance now that further, independent spectropolarimetric observations of EZ CMa be obtained at high resolution. We also hope that our results will stimulate additional theoretical studies of polarized radiation transfer in rotating, expanding, nonspherical atmospheres so that calculated polarized line profiles can be matched with observations.

We are grateful to the dedicated team that supports Pine Bluff Observatory. We particularly want to thank M. R. Meade, B. Babler, A. J. MacDonald, K. H. Strobel, M. J. Wolff, and G. Tiede for helping with the observations and reductions. This work was supported by NASA contract NAS5-26777.

REFERENCES

Cassinelli, C. P., and Haisch, B. M. 1974, *Ap. J.*, **188**, 101.
Castor, J. I., Abbott, D. C., and Klein, R. I. 1975, *Ap. J.*, **195**, 157.
Cropper, M., Bailey, J., McCowage, J., Cannon, R. D., Couch, W. J., Walsh, J. R., Strade, J. O., and Freeman, F. 1988, *M.N.R.A.S.*, **231**, 695.
Drissen, L., Robert, C., Lamontagne, R., Moffat, A. F. J., St.-Louis, N., van Weeren, N., and van Genderen, A. M. 1989, *Ap. J.*, **343**, 426.
Firmani, C., Koenigsberger, G., Bisiacchi, G. F., Moffat, A. F. J., and Isserstedt, J. 1980, *Ap. J.*, **239**, 607.
Hartmann, L., and Cassinelli, J. P. 1977, *Ap. J.*, **215**, 155.
Hillier, D. J. 1984, *Ap. J.*, **280**, 744.
———. 1987, *Ap. J. Suppl.*, **63**, 965.
Kuhi, L. V. 1967, *Pub. A.S.P.*, **79**, 57.
Lamontagne, R., Moffat, A. F. J., and Lamarre, A. 1986, *A.J.*, **94**, 1008.
Maeder, A. 1987, *Astr. Ap.*, **178**, 159.
McLean, I. S. 1980, *Ap. J. (Letters)*, **236**, L149.
McLean, I. S., Coyne, G. V., Frecker, J. E., and Serkowski, K. 1979, *Ap. J. (Letters)*, **231**, L141.
Nordsieck, K. H. 1987, *Bull. AAS*, **19**, 1098.
———. 1991, in preparation.
Pauldrach, A., Puls, J., Hummer, D. G., and Kudritzki, R. P. 1985, *Astr. Ap.*, **148**, L1.
Poe, C. H., Friend, D. B., and Cassinelli, J. P. 1989, *Ap. J.*, **337**, 888.
Poeckert, R., and Marlborough, J. M. 1978, *Ap. J.*, **220**, 940.
Robert, C., Moffat, A. F. J., Drissen, L., Lamontagne, R., and Seggewiss, W. 1990, in *IAU Symposium 143, Wolf-Rayet Stars and Interrelations with Other Massive Stars in Galaxies* (Dordrecht: Reidel), in press.
Serkowski, K. 1970, *Ap. J.*, **160**, 1083.
Willis, A. J., Howarth, I. D., Smith, L. J., Garmany, C. D., and Conti, P. S. 1989, *Astr. Ap. Suppl.*, **77**, 269.
Wilson, O. C. 1948, *Pub. A.S.P.*, **60**, 383.

C. M. ANDERSON, K. S. BJORKMAN, A. M. MAGALHÃES, M. A. NOOK, K. H. NORDSIECK, R. E. SCHULTE-LADBECK, and M. TAYLOR: Space Astronomy Laboratory, The University of Wisconsin at Madison, 1150 University Avenue, Madison, WI 53706